Performance of Coreless-Winding Axial-Flux Permanent-Magnet Generator With Power Output at 400 Hz, 3000 r/min

Federico Caricchi, *Member, IEEE*, Fabio Crescimbini, *Member, IEEE*, Onorato Honorati, *Member, IEEE*, Giulia Lo Bianco, and Ezio Santini, *Member, IEEE*

***Abstract*— An axial-flux permanent-magnet machine (AFPM) topology with coreless winding is proposed for generator units required aboard ships, aircraft, or hybrid electric vehicles. In the proposed AFPM configuration, the winding consists of rhomboidal-shaped coils encapsulated in fiber-reinforced epoxy resin. The coils have a double-layer arrangement to leave space for a cooling water duct being used to remove heat directly from the interior surface of the winding. The overall machine structure has high compactness and lightness and, due to the lack of the iron core, generator operation with power output at 400 Hz can be accomplished with high efficiency and acceptable voltage regulation. This paper discusses the basic design and construction of AFPM generators with coreless winding and experimental results taken from a 16-pole machine prototype rated 230 N·m, 3000 r/min are finally reported.**

***Index Terms*— Aerospace power generation, on-board electric generators, permanent-magnet machines.**

I. Introduction

In THE DESIGN of electric machinery for power generation aboard ships, aircraft, or hybrid electric cars and buses, considerable efforts are made to ensure that compactness and lightness are as high as possible. Other factors, such as material cost or manufacturing convenience, which may be of prime importance for conventional generators, are relatively minor considerations, because savings in generator weight and size can be repaid by substantial fuel economies or improvements in payload capability for the complete vehicle. Because of the high compactness and lightness required, to date, synchronous machines with Nd–Fe–B permanent-magnet (PM) excitation are the most suitable candidates for such a generator application. Compared to machines having adjustable field excitation, PM generators have the potential disadvantage of a poor voltage regulation, but this problem can be easily overcome by using electronic circuits for power conditioning.

Within the broad category of PM machines, several distinct magnetic circuit configurations can be identified. These include the axial-flux permanent-magnet machine (AFPM) topology, which has been under investigation in the past [1]–[8] and, in the last few years, has received renewed interest concerning various machine applications, such as wheel motor drives [9] and portable generator sets [10].

Among the AFPM topologies which have been investigated more recently, a machine configuration with coreless winding sandwiched between two PM rotor discs was proposed [11], [12] for use in a prototype of wheel direct drive [13]. Such an AFPM arrangement has similarity with the PM ac disc motor presented in [6] and basically is a brushless machine version of the well-known disc-armature or printed-circuit dc motor which, in the past, has been widely used in servomotor applications requiring fast-response dynamics [1]–[5]. However, unlike such earlier disc-shaped machines, an original feature of the AFPM topology discussed in [11]–[13] is the use of rhomboidal-shaped coils having suitable arrangement to leave space for a cooling water duct. Thereby, heating due to the power losses in the machine winding is directly removed from the interior surface of the winding coils, and this allows totally enclosed construction and long-term operation with high overloads.

The AFPM topology with water-cooled rhomboidal-shaped coils proved to be particularly suitable for the in-wheel motor application, as high compactness and lightness are achieved. On the other hand, it is found that the lack of the iron core and, thereby, of the power loss inevitably associated to any iron circuit subject to a time-variable magnetic field, allows generator operation with substantially high efficiency, even though power output at relatively high frequency is required. In addition, generator operation with acceptable voltage regulation is achieved due to a negligible armature reaction, this being a consequence of the very low value of the machine inductance which results from the ironless arrangement of the winding. Thereby, a novel application of the AFPM topology which was initially investigated for use in wheel direct drives is envisaged concerning the light and compact generator units being required for power generation at 400 Hz. In consideration of that, this paper discusses design and construction of AFPM generators having coreless winding

Paper IPCSD 98–46, presented at the 1997 Industry Applications Society Annual Meeting, New Orleans, LA, October 5–9, and approved for publication in the IEEE TRANSACTIONS ON INDUSTRY APPLICATIONS by the Electric Machines Committee of the IEEE Industry Applications Society. Manuscript released for publication June 29, 1998.

F. Caricchi, F. Crescimbini, O. Honorati, and E. Santini are with the Department of Electrical Engineering, University of Rome "La Sapienza," 00184 Rome, Italy.

G. Lo Bianco was with the Department of Electrical Engineering, University of Rome "La Sapienza," 00184 Rome, Italy. She is now with ENEA C.R.E. Casaccia, 00060 Santa Maria di Galeria, Rome, Italy.

Publisher Item Identifier S 0093-9994(98)08109-2.

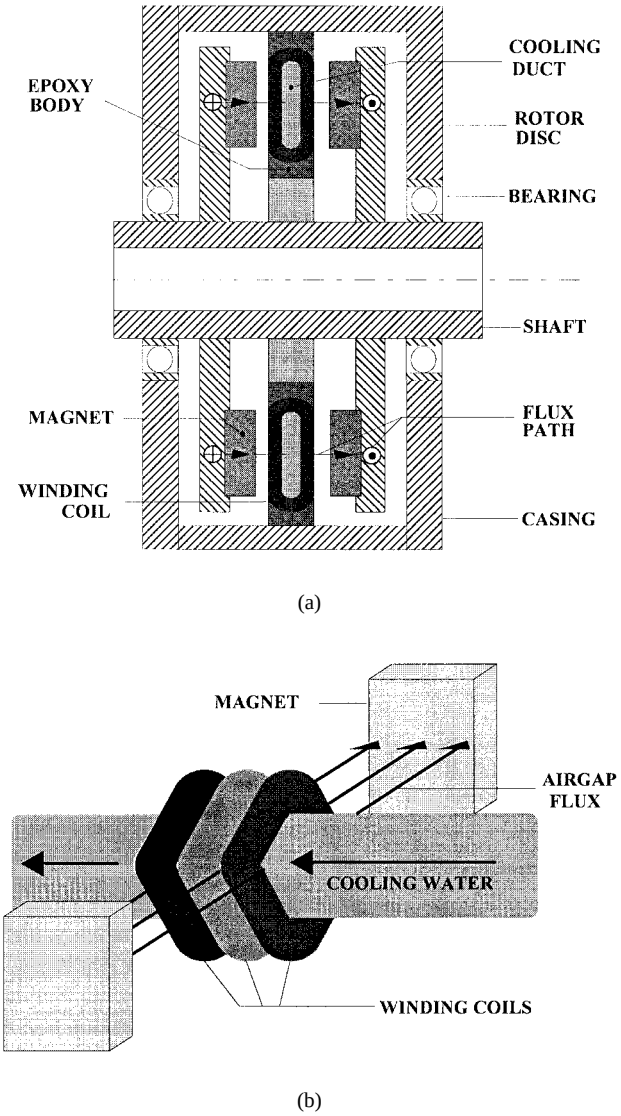

Fig. 1. AFPM with coreless winding. (a) Cross section of the machine layout. (b) Machine cooling arrangement.

with rhomboidal-shaped coils. Experimental results taken from a 16-pole machine prototype rated 230 N·m, 3000 r/min are finally reported.

II. Machine Structure

Fig. 1(a) shows a cross section of the basic layout of an AFPM with coreless winding. Because of the lack of the toroidal core, the flux driven by the magnets is to pass axially from a north pole on one rotor to a facing south pole on the other, as depicted in Fig. 1(b). Thereby, the machine has quite a large airgap, comprising the winding thickness and running clearance on either side of it. The winding coils are located toward the middle of this airgap and lie on the transverse plane normal to the machine shaft. The interaction between the airgap flux driven by the magnets and the current flowing in the winding coils results in a tangential force on each conductor and, thereby, all together, these forces produce the machine torque. In the proposed machine layout, the winding coils have rhomboidal shape and space is left between the two active

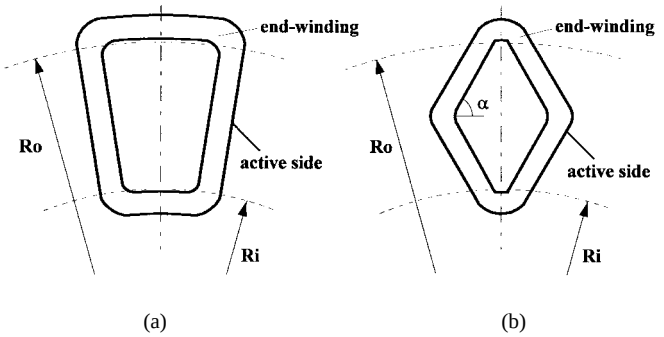

Fig. 2. Coil shapes for AFPM's with coreless winding. (a) Trapezoidal coil. (b) Rhomboidal coil.

sides of each coil for giving a path to cooling water. Heating due to I^2R and eddy–current loss in the winding is thereby removed by a water flow being forced to pass through the coils, as shown in Fig. 1(b).

The torque generated at the airgap is mainly a function of the machine outer diameter. If the available space is too small in diameter, then the required torque can be achieved by means of a multistage machine arrangement. In a multistage machine, j being the number of stages, the machine has j three-phase windings and $(j+1)$ PM disc rotors. The $(j+1)$ rotors share a common mechanical shaft, whereas the terminals of the j windings may be connected either in series or parallel among them. In multistage machines, only the two external rotor discs must be made of material with good magnetic properties (typically, mild steel), since they are used to provide a return path for the main flux. The intermediate rotors, on the other hand, are used merely for mechanical support of the magnets, so that lightweight nonmagnetic materials (e.g., aluminum) can be used for their construction, thus enhancing the machine compactness and lightness [13].

III. Design Fundamentals

A. Shape of the Winding Coils

As in the earlier disc-shaped machines with ironless winding [1]–[6], the winding coils may have the trapezoidal shape shown in Fig. 2(a). This coil shape allows the maximum coil flux linkage, as each coil embraces the entire pole area, but, on the other hand, the coil end windings necessitate a three-tier arrangement and may have significant length if compared with the length of the conductor active sides. Therefore, disregarding the case of machines having a very large number of poles and, thereby, very short end windings, the use of trapezoidal coils negatively affects the value of torque produced per unit of I^2R, and this is undesirable for machine applications with high power ratings.

As discussed in [12], higher values of torque per unit of I^2R can be achieved if the winding coils have the rhomboidal shape shown in Fig. 2(b). In fact, due to the inclined arrangement of the coil active sides, in rhomboidal coils, the end windings are greatly shortened, but with only a small reduction of the coil flux linkage if compared with the conventional trapezoidal-shape coils. In addition to that, the

use of rhomboidal coils allows a two-tier arrangement of the end windings with consequent reduction of the winding axial thickness and simplification of manufacturing.

The geometry of rhomboidal coils is characterized by the inclination angle α and the ratio K_r between the inner radius R_i and outer radius R_o. For given values of the outside diameter and of the magnetic and electric loadings, machine characteristics such as torque, torque-to-weight ratio, and efficiency are greatly affected by the coil geometry. Hence, the machine design optimization process primarily consists of selection of suitable values for both α and K_r. With the values of α and K_r related to an optimized design, it is found that the use of rhomboidal coils results in 25%–30% reduction of winding resistance and 10%–12% reduction of EMF, compared to trapezoidal coils.

B. EMF Waveform

The EMF is nearly sinusoidal, whereas iron-cored AFPM's tend to produce a trapezoidal EMF. The sinusoidal waveform is the result of using short-pitch distributed coils as in a conventional three-phase ac winding and of the rhomboidal coil shape which further suppresses harmonics in the same way as skewed or herringbone coils. Both the flux density distribution at the machine airgaps and the coil geometry influence the peak value of the induced EMF and, thereby, the machine torque.

C. Machine Torque

The electromagnetic torque developed at the machine airgaps can be expressed as

$$T = k_t \cdot \pi \cdot J \cdot B \cdot R_o^3 \cdot K_r \cdot (1 - K_r^2) \tag{1}$$

where J is the electric loading at the radius R_i, B is the peak flux density of an ideal square-wave distribution at the machine airgaps, k_t is a machine constant which depends on both the actual airgap flux-density distribution and the coil geometry being utilized. For any particular machine design, the constant k_t can be viewed as the per-unit torque referred to the torque of the same machine, but having square-wave flux-density distribution and concentrated full-pitch coils.

Due to flux leakage and fringing, the flux density at the airgaps is not a square wave in distribution and, therefore, whatever coil geometry is being used, it is found that $k_t < 1$. On the other hand, compared to the conventional trapezoidal coils, rhomboidal coils result in a further reduction of k_t, as the peak of the EMF induced in the machine winding is substantially affected by the inclination of the coil active conductors. For the purpose of machine design, first-tentative values of k_t as a function of the inclination angle α can be determined by assuming a square-wave distribution of the airgap flux density. It is found that a maximum value of k_t actually does exist, and this is achieved with a particular value of α which depends on the selected value of K_r [12].

D. I^2R Power Loss

In a rhomboidal coil, the length of the conductors depends on K_r and α and, therefore, these parameters affect the I^2R loss of winding coils. For a fixed value of K_r, the coil resistance can be expressed as a function of α and then given in per unit with respect to the resistance of a trapezoidal coil which has the same value of K_r. Such design calculations show that the I^2R loss of rhomboidal coils decreases as α increases and, thereby, benefits would arise from values of α as high as possible. On the other hand, the higher values of α lead to an undesirable decrease of k_t and, thereby, of the machine torque. A compromise value of α is needed, and it is found that the best design approach is based on the minimization of the ratio between I^2R loss and torque [13].

E. Eddy-Current Power Loss

The winding is located in the airgap and, hence, is situated in the main field. Motion of the magnets past the winding causes the field through each conductor to vary periodically and to induce eddy currents. The loss due to eddy currents in the conductors depends on both the geometry of the wire cross section and the waveform of the flux density variation.

Round wires are less prone to eddy currents, but they have a worse fill factor compared to rectangular conductors. Hence, in cases where the phase current is large, the use of rectangular-section conductors is unavoidable and, thereby, a conductor arrangement consisting of either Litz wires or thin wide rectangular-shaped conductors is to be adopted to lower the high eddy-current loss that otherwise would occur. Litz wires allow a great reduction of the eddy-current loss, but they are much more expensive and have much lower fill factor compared to solid wire conductors. On the other hand, provided that the field through conductors has negligible component of flux density in the direction orthogonal to the conductor width, the use of copper-strip conductors with a thickness of 1 mm, or even below that, allow a low-cost conductor arrangement where the total winding loss, i.e., I^2R and eddy current, is reduced to an acceptable value.

Sinusoidal variation of uniform field through rectangular-section conductors gives rise to eddy-current loss per unit volume

$$P_{ec} = (B_{pk} \cdot \omega \cdot \delta)^2/(24 \cdot \rho) \tag{2}$$

where B_{pk} is the peak flux density of a sinusoidal distribution, ω is the electrical angular frequency, δ is the conductor thickness, and ρ is the conductor resistivity at the winding working temperature. In AFPM's, however, the flux density distribution at the airgap is much closer to a trapezoidal waveform with significant harmonic content of third and fifth, although fringing of flux at the edges of the poles contributes to lower the amplitude of the higher harmonics. Further to that, in a machine with coreless winding arrangement, the field through each conductor has tangential component of flux density, which can lead to serious additional eddy-current loss. Taken together, these features lead to eddy-current power loss greater than the one resulting from (2) and, thereby, for the purpose of design and performance calculations, the loss found from (2) is to be multiplied by an empirical factor obtained through a finite-element study of the distribution of flux density at the airgap.

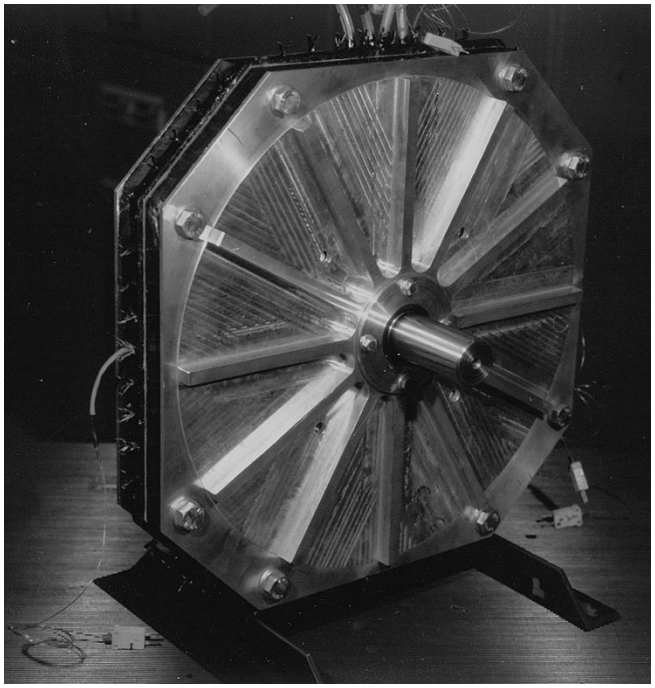

Fig. 3. Machine prototype rated 70 kW at 3000 r/min.

TABLE I
LEADING CHARACTERISTICS OF THE PROTOTYPE MACHINE

Number of poles	16	
Rated torque	230	Nm
Peak torque	460	Nm
Phase peak EMF (@ 3000 rpm)	224	V
Peak airgap flux density	0.6	T
Machine phases	3	
Winding coils	48	
Outer diameter	400	mm
K_r	0.6	
α	60°	
Number of turns per coil	16	
Conductor dimensions (copper strip)	4mm x 0.65mm	
Winding electric loading	77	kA/m
Cooling water flow	5	l/min
Phase resistance (@ 20°C)	25.6	mΩ
Phase self inductance	84	μH
Machine axial length	53	mm
Stator weight	5.5	kg
Rotor weight (without PMs)	15	kg
PM weight	6.5	kg
Machine total weight	42	kg

F. Design Criteria

From design optimization studies, it is found that K_r mainly influences torque and torque-to-weight ratio, whereas it has a small impact on the machine efficiency. For given outside diameter and loadings, the torque is maximized if K_r is set equal to $1/\sqrt{3}$, but, in most designs, the maximum torque-to-weight ratio is achieved at a slightly higher value of K_r. Therefore, for K_r, a compromise value is required to be generally found in the range from 0.6 to 0.7.

On the other hand, the angle α greatly affects the machine efficiency because of the influence on both the torque and the I^2R loss, as previously discussed. Hence, for a given value of K_r, the machine efficiency is maximized if α is chosen to result in I^2R loss as low as possible without producing significant reduction of the torque. For most machine designs, an optimum value of α is generally found in the range from 60° to 70°.

IV. MACHINE PROTOTYPE

Fig. 3 shows an external view of a prototype of an AFPM with coreless winding which was initially constructed with the aim of testing the novel winding arrangement with water-cooled rhomboidal coils [13]. This machine has axially polarized rectangular slabs of Nd–Fe–B material being mounted on the surface of soft-iron disc rotors. The remanence of the PM grade used is approximately 1.3 T and the coercivity is approximately 1000 kA/m. The winding consists of 48 rhomboidal coils wound from rectangular copper strip. To achieve the machine stator as it stands in its final form, the winding coils are placed side by side in a toroidal fashion and then encapsulated with fiberglass-reinforced epoxy resin to form a rigid body. Owing to the particular method being used for encapsulating the winding with epoxy, in the prototype machine, a 4-mm-thick toroidal duct is left between the active sides of the coils. This toroidal duct is used for providing cooling of the machine winding through pump-assisted circulating water. Due to the prototype nature of the above-described AFPM generator, thermocouples for monitoring temperature were placed at several points within the winding.

Table I summarizes the leading characteristics of the above-described prototype machine, which actually was designed having in mind motoring operation in a wheel direct drive with base speed at 750 r/min. For this application, all the winding coils were connected in series among them, but to the aim of testing the machine at 3000 r/min, it was found suitable to modify the connection of the winding coils to keep the open terminal voltage at its original value. Hence, generator operation with power output at 400 Hz was tested with the machine winding being formed of four paralleled paths.

V. 400-Hz GENERATOR PERFORMANCE

Testing of the prototype machine operation with power output at 400 Hz required the arrangement of a test rig, as schematically depicted in Fig. 4. Hence, laboratory tests were devoted to evaluate generator performance concerning no-load operation with variable speed up to 3000 r/min and machine load conditions at 3000 r/min under either three-phase resistive load or diode rectifier with adjustable dc load.

A. No-Load Tests

Tests were initially carried out driving the machine at open terminals to display the machine EMF waveform and determine the no-load power loss from the measurement of the

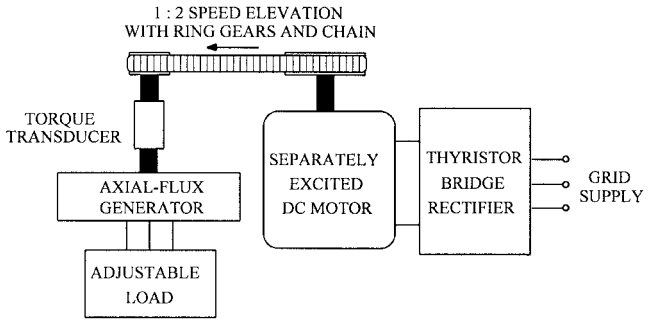

Fig. 4. Test rig arrangement.

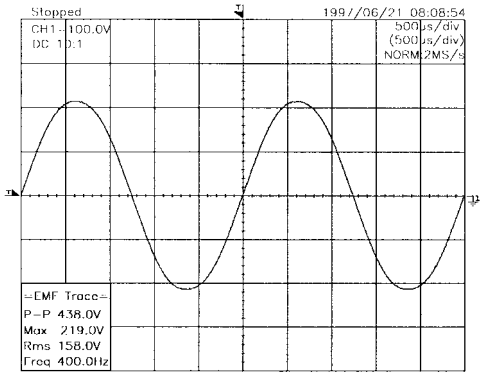

Fig. 5. Oscilloscope trace of the prototype machine EMF waveform (time scale: 500 μs/div; voltage scale: 100 V/div).

input torque required to operate the machine at a given speed. In order to evaluate whether circulating currents would occur in the winding paralleled paths as a result of incidental EMF dissimetries due to machine manufacturing, measurement of the no-load power loss was carried out with the terminals of the winding paths being either disconnected one from the other or paralleled among them. However, these two arrangements of the winding terminals resulted in very close values of the measured input torque and, thereby, it was concluded that no circulating currents actually occur in the winding paths when paralleled.

Fig. 5 shows the waveform of the open terminal voltage measured at 3000 r/min. According to design predictions, the EMF should be sinusoidal with negligible harmonic content and, at 400 Hz, the measured peak value is about 2% less than the figure of 224 V resulting from design calculations.

As the machine winding has an ironless arrangement, only the eddy-current loss together with frictional and aerodynamic losses constitute the no-load loss of the generator. In principle, all these losses vary according to the square of the speed, although at the no-load condition any increase of the machine speed produces an increase of the winding temperature which results in a lower than expected eddy-current loss due to a higher value of the copper resistivity. To consider such an aspect, measurements of the machine input torque were taken starting from the nominal condition of 3000 r/min and then reducing the generator speed, so that it was possible to achieve a set of data referred to an almost constant winding

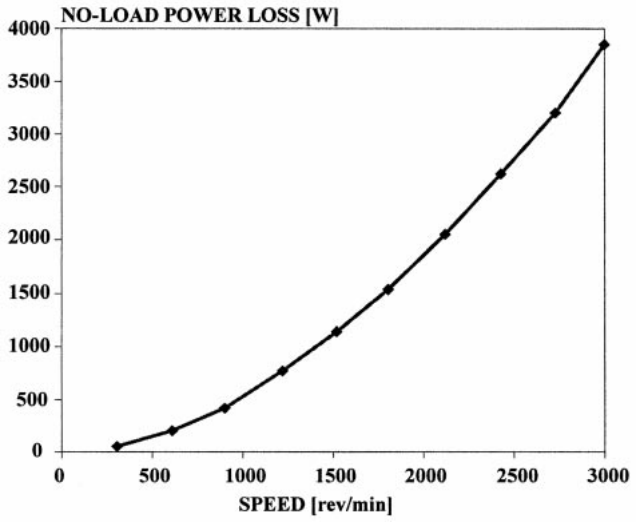

Fig. 6. No-load power loss of the test generator running at various speeds.

temperature of 45 °C. Fig. 6 gives results of the generator no-load tests in terms of shaft input power measured along a wide range of running speeds. It is found that, at 3000 r/min, the test generator has no-load power loss of approximately 3.8 kW, i.e., 5% of the nominal power output of the machine when loaded at 3000 r/min with the rated torque.

B. Load Tests

The machine torque is proportional to the load current and the rated torque of the test generator is achieved with three-phase sinusoidal output current of 152-A rms. Hence, at 3000 r/min, the prototype machine is capable of working out continuous input power of about 72 kW. Load tests included running conditions with short-circuited winding terminals and output frequency in the range of a few hertz. Because of the very low speed used, the input torque measured in such a short-circuit condition is proportional to the winding I^2R loss and, thereby, from the measurement of the output rms current, a mean value of the winding phase resistance can be determined. At working temperature of about 45 °C, the phase resistance of the test generator was found to be about 29 mΩ. This value is close to the design prediction and has been used for the calculation of generator efficiencies at several values of load current. It is found that, at both nominal load and 100% overload conditions, the machine efficiency is close to 92%, whereas the test generator has maximum efficiency of about 93% somewhere around the 150% overload condition. This is an odd feature which is due to a higher than expected loss at no load.

Concerning the use of PM machines as generators, the output voltage regulation is one critical performance requirement, as there is no excitation control to compensate the voltage drop caused by the load current. Because of a very low machine inductance, AFPM's with coreless winding have rms output voltage which varies almost linearly with load current. This clearly appears from Fig. 7, which refers to data achieved from operations at constant speed of 3000 r/min and under diode bridge rectifier with various values of the dc load. From

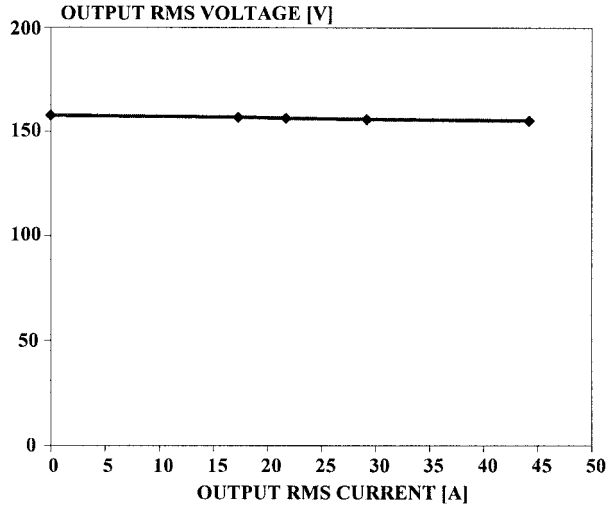

Fig. 7. Output voltage regulation of the test generator running at 3000 r/min and with various loads.

the slope of the measured characteristic, it is found that the test generator has percentage voltage regulation of about 6% from no-load to full-load current.

C. Assessment of Test Results

Taken as a whole, the measured performance of the test generator are substantially satisfactory, even though at the nominal speed of 3000 r/min the no-load loss is rather serious because of the very high eddy currents induced in the winding. This, however, was not a surprise, as from tests carried out at 750 r/min [13], a no-load loss of about 250 W was found and, thereby, the no-load loss measured at 400 Hz is just the loss amount one should expect from running the machine at a speed four times higher than the machine design speed. Notwithstanding this, the tests carried out at 400 Hz have brought to light a serious additional eddy-current loss due to the tangential component of the airgap flux density. In fact, due to the coreless arrangement of the winding, at the pole edges, the tangential component of the airgap flux density has a significant value, as it clearly appears from Fig. 8, which shows results of a finite-element study conducted by considering the actual airgap geometry of the test generator. Hence, the presently adopted winding arrangement is unlikely to be suitable for 400-Hz output operation, and some form of two-tier construction of the conductors is needed. It has been calculated that simply splitting the strips into two pieces 2-mm high would be sufficient in the present generator to substantially reduce the eddy-current loss due to the tangential component of the airgap flux density and achieve maximum efficiency of 94.3% at the full-load current.

The use of finely divided strands would drastically reduce the eddy-current loss, but, on the other hand, would also inevitably result in an increase of the I^2R loss because of the much lower fill factor compared to solid wire conductors. As an example, if Litz wires were used in the generator prototype, the eddy-current loss would become practically negligible, but the I^2R loss would be 2.5–3 times higher than the present value because of a fill factor being in the range from 0.55 to

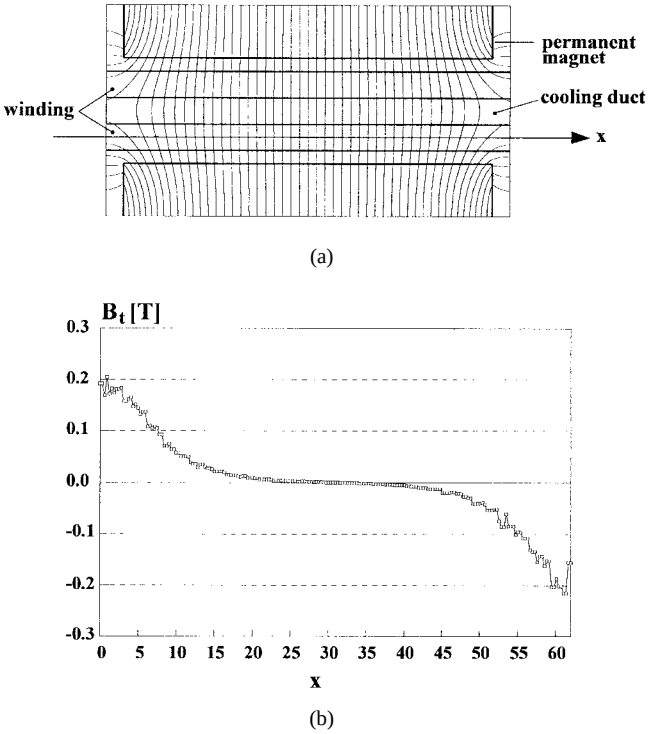

Fig. 8. Flux density distribution along one pole pitch: (a) field map and (b) tangential component B_t of the airgap flux density.

0.65. In this case, the prototype machine would have full-load efficiency on the order of 92%–93%, although much higher efficiency values would be achieved at light load conditions. Hence, it clearly appears that a compromise choice is needed for the conductors of an airgap winding, and for the prototype generator, it is calculated that full-load efficiency slightly exceeding 95% may be achieved with a conductor arrangement which minimizes the sum of the I^2R and eddy-current losses.

VI. Conclusions

Because of the high compactness and lightness required, power generation aboard ships, aircraft, or hybrid electric vehicles is better accomplished with electric machines operated with 400-Hz power output and, concerning such a generator application, this paper has concerned the use of AFPM's having coreless winding. Basic aspects of the machine design have been discussed, and laboratory results taken from a general-purpose test generator have been reported to show that satisfactory performance can be achieved, even though the machine has nonoptimized design in terms of conductor arrangement. This allows the conclusion that the combination of the new high-field PM's with the proposed machine layout makes for a very compact machine which has extremely high torque-to-weight ratio. Of course, because of the use of an ironless winding immersed in a high-frequency rotating field, the eddy-current loss is a serious difficulty, but it is believed that in machines purposely designed for application in 400-Hz power generation, this problem can be quite easily solved by using conductor arrangements based on Litz wires or multitier construction of the conductors.

REFERENCES

[1] P. Campbell, "Principles of a permanent magnet axial-field D.C. machine," *Proc. Inst. Elect. Eng.*, vol. 121, no. 12, pp. 1489–1494, Dec. 1974.

[2] P. Campbell, D. J. Rosenberg, and D. P. Stanton, "The computer design and optimization of axial-field permanent magnet motors," *IEEE Trans. Power App. Syst.*, vol. PAS-100, pp. 1490–1497, Apr. 1981.

[3] G. R. Slemon and A. Straughen, *Electric Machines.* Reading, MA: Addison-Wesley, 1980, pp. 335–336.

[4] A. E. Fitzgerald, C. Kingsley, and S. Umans, *Electric Machinery.* New York: McGraw-Hill, 1990, pp. 523–524.

[5] G. Henneberger, H. Harer, S. Schustek, and L. Verstege, "A new range of DC and AC pancake motors," in *Proc. Int. Conf. Electrical Machines*, 1986, pp. 916–919.

[6] G. B. Kliman, "Permanent magnet AC disc motor electric vehicle drive," presented at SAE Int. Congr. Exposition, Detroit, MI, Feb. 28–Mar. 4, 1983.

[7] W. S. Leung, and J. C. C. Chan, "A new design approach for axial-field electrical machines," *IEEE Trans. Power App. Syst.*, vol. PAS-99, pp. 1679–1685, July/Aug. 1980.

[8] C. C. Chan, "Axial-field electrical machines—Design and applications," *IEEE Trans. Energy Conversion*, vol. EC-2, pp. 294–300, June 1987.

[9] F. Caricchi, F. Crescimbini, E. Fedeli, and G. Noia, "Design and construction of a wheel-directly-coupled axial-flux PM motor prototype for EV's," in *Conf. Rec. IEEE-IAS Annu. Meeting*, 1994, vol. I, pp. 254–261.

[10] E. Spooner and B. J. Chalmers, "TORUS—A slotless toroidal-stator, permanent magnet generator," *Proc. Inst. Elect. Eng.*, vol. 139, pt. B, pp. 497–506, Nov. 1992.

[11] F. Caricchi, F. Crescimbini, and E. Santini, "Optimum design of ironless stator winding for axial-flux PM machines," in *Proc. IEE 6th Int. Conf. Electrical Machines and Drives*, Oxford, U.K., Sept. 8–10, 1993, pp. 652–658.

[12] F. Caricchi and F. Crescimbini, "Axial-Flux permanent-magnet machine with water-cooled Ironless stator," in *Proc. IEEE Power Technology Conf.*, Stockholm, Sweden, June 18–22, 1995, pp. 98–103.

[13] F. Caricchi, F. Crescimbini, F. Mezzetti, and E. Santini, "Multi-stage axial-flux PM machine for wheel direct drive," *IEEE Trans. Ind. Applicat.*, vol. 32, pp. 882–888, July/Aug. 1996.

Federico Caricchi (M'90), for a photograph and biography, see p. 116 of the January/February 1998 issue of this TRANSACTIONS.

Fabio Crescimbini (M'90), for a photograph and biography, see p. 116 of the January/February 1998 issue of this TRANSACTIONS.

Onorato Honorati (M'73), for a photograph and biography, see p. 116 of the January/February 1998 issue of this TRANSACTIONS.

Giulia Lo Bianco received the Degree in electrical engineering and the Ph.D. degree from the University of Rome "La Sapienza," Rome, Italy, in 1992 and 1998, respectively.

She is currently with ENEA C.R.E. Casaccia, Rome, Italy. Her research interests are renewable-energy generating systems and generator application of permanent-magnet machines.

Ezio Santini (M'91) was born in Rome, Italy, in 1956. He received the Degree in electrical engineering (cum laude) from the University of Rome "La Sapienza," Rome, Italy, in 1982.

From 1983 to 1990, he was an Assistant Professor in the Department of Electrical Engineering, University of Rome "La Sapienza," and, since 1991, he has been an Associate Professor of Design of Electromagnetic Devices. His research activities are in the fields of electrical machines models, transient phenomena in transformers and rotating machines, FEM analysis of electromagnetic fields in electrical devices, and numerical methods in electrical engineering.

Prof. Santini is a member of the Italian Association of Electric and Electronics Engineers and the IEEE Power Engineering Society.